Absence of Andreev reflections and Andreev bound states above the critical temperature

Y. Dagan, A. Kohen, and G. Deutscher
School of Physics and Astronomy, Raymond and Beverly Sackler Faculty of Exact Sciences, Tel Aviv University, 69978 Tel Aviv, Israel

A. Revcolevschi
Laboratoire de Chimie des Solides, Universite Paris–Sud, 91405 Orsay, France
(Received 9 July 1999)

We present measurements of the temperature dependence of the differential conductance of normal-metal/underdoped high-T_c superconductors contacts. Both $Y_1Ba_2Cu_3O_{7-x}$ thin films and $La_{2-x}Sr_xCuO_4$ single crystals were studied. The effect of direct Andreev reflections, or of Andreev bound states, do not persist above the critical temperature. Our results are consistent with an Andreev energy scale that does not follow the doping dependence of the pseudogap, but rather that of the critical temperature.

I. INTRODUCTION

Andreev reflection[1] is a phenomenon which occurs at the boundary between a superconductor and a normal metal. It was originally developed to explain the thermal conductivity across such a boundary, and later used to explain the electrical conductance of a normal-metal/superconductor weak link. If we look at an electron propagating in the normal metal with an energy, measured from the Fermi level, lower than the superconductor's energy gap, it cannot enter the superconductor as a quasiparticle excitation. However, it can enter the superconducting condensate in the following way: a hole with opposite momentum is reflected into the normal metal and an electron pair is added to the condensate. This results in a conductance twice as big as the normal conductance (conductance at energies much higher than the energy gap of the superconductor). Later, Blonder, Tinkham, and Klapwijk (BTK) (Ref. 2) considered the case of normal-metal/superconductor (NS) contact with a barrier between the two electrodes, and calculated the conductance for intermediate cases ranging from a clean NS contact to a normal-metal/insulator/superconductor (NIS) tunneling contact. Kashiwaya *et al.*[3] expanded BTK's calculation for the case of a gap having a *d*-wave symmetry. They showed that another feature, absent in BTK's calculation, is expected for the case where the order parameter changes sign along the electron's trajectory: a zero-bias conductance peak (ZBCP), due to Andreev surface bound states.

In the BCS theory, the order parameter decreases as the temperature is raised, and vanishes at the critical temperature. For low T_c materials this was found experimentally to be the case. In high-temperature superconductor (HTS) materials the situation is not clear. For example, scanning tunneling microscope (STM) measurements made by Renner *et al.*[4] on underdoped $Bi_2Sr_2Ca_1Cu_2O_{8+\delta}$ (2212) show a nonvanishing gap above T_c, and the value of the gap seems to be constant below T_c. This has been explained by a pseudogap existing in HTS above T_c. The nature of this pseudogap is unsettled at the present time. On the one hand, it has been suggested that it is a special normal-state property of the HTS,[5] but on the other hand it has been proposed that it is a signature of preformed incoherent Cooper pairs,[6] or of a spin pairing amplitude,[7] above T_c. Recently, Choi *et al.*[8] have predicted that even for the case of preformed incoherent Cooper pairs, Andreev reflections should occur above T_c, as they do for the coherent pairs of the condensate below T_c. Choi *et al.* suggest that this phenomenon can be probed more easily in heavily underdoped materials, due to the relatively high temperatures at which the pseudogap appears. Assuming their prediction to be correct, a measurement of the differential conductance as a function of temperature below and above T_c for underdoped samples, should be able to determine whether there are preformed incoherent pairs above T_c, or not. We show here that the Andreev reflections disappear in fact at T_c for underdoped $YBa_2Cu_3O_{7-x}$ (YBCO) and $La_{2-x}Sr_xCuO_4$ (LSCO) junctions.

II. SAMPLE PREPARATION, CHARACTERIZATION, AND MEASUREMENTS

YBCO *c*-axis oriented thin films were grown by rf off-axis magnetron sputtering. Samples Y1 to Y8 were grown on $SrTiO_3$ and $LaAlO_3$ substrates, using a pressure template.[9] The growth temperature was 770 °C and the pressure 400 mTorr. A magnetic measurement of the critical temperature of a film grown in such conditions is presented in Fig. 1

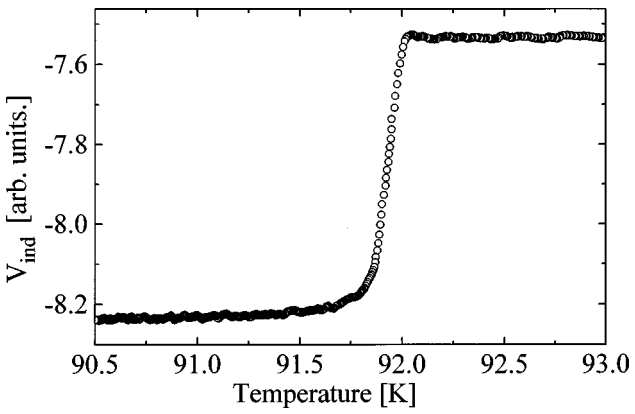

FIG. 1. Magnetic induction measurement of T_c for YBCO film. $T_c = 91.85$ K with a width of $\Delta T_c = 0.15$ K.

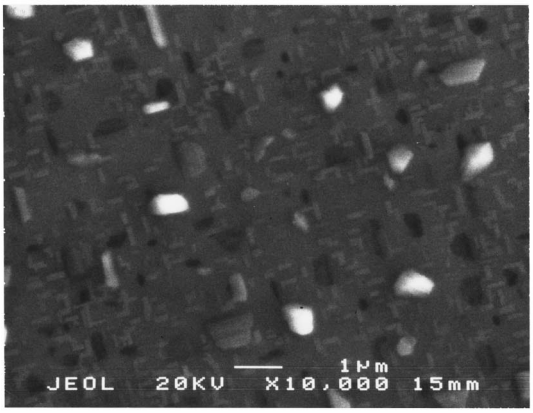

(a)

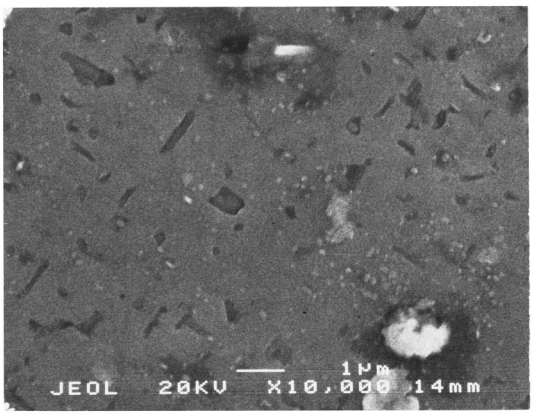

(b)

FIG. 2. Scanning electron microscope pictures of our YBCO samples. (a) YBCO film with *a*-axis grains corresponding to the samples of group I (samples Y1–Y4, Y8). (b) YBCO film with almost no *a*-axis grains but with small holes corresponding to the samples of group II (samples Y5–Y7).

(sample Y7). The critical temperature shown is $T_c = 91.85\,\mathrm{K}$ with a width $\Delta T_c = 0.15\,\mathrm{K}$. X-ray Bragg diffraction was performed on the YBCO films. Samples Y1–Y4, Y8 (group I) are *c*-axis oriented films with less than 5% *a*-axis grains. They are easily detected by a scanning electron microscope (SEM). Samples Y5–Y7 (group II) exhibit no traces of an *a* axis in the x ray; however, upon checking these samples in the SEM, holes of the order of 0.5 μm and a few *a*-axis grains can be seen on the film surface.They are much smaller than those in the previous group of samples. In Fig. 2 we present two SEM pictures of our YBCO films. Fig. 2(a) corresponds to a YBCO film with *a*-axis grains, characteristic of samples of group I, and Fig. 2(b) corresponds to the YBCO films on which the samples of group II were fabricated.

A single crystal of $La_{2-x}Sr_xCuO_4$ with $x = 0.12$ was grown in an image furnace by a vertical traveling solvent zone method using feed rods prepared by pressing and sintering appropriate mixtures of La_2O_3, $SrCO_3$, and CuO of purity higher than 99.99%. Growth was carried out at a growth rate of 1 mm/h resulting in single crystals several cm long. Single crystallinity was checked by neutron diffraction and rocking curves were performed about the axis of the crystals, indicating half width at half maximum of less than 20′, a sign of high crystalline quality.

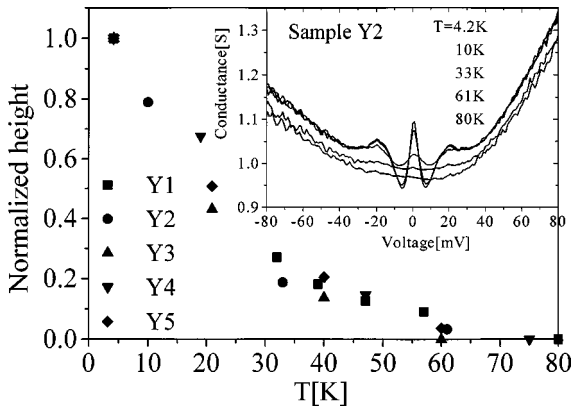

FIG. 3. Height of the ZBCP at various temperatures normalized with the height of the ZBCP at 4.2 K for Samples Y1–Y5. (YBCO) Inset: plot (Sample Y2) of conductance versus voltage at temperatures 4.2, 10, 33, 61, and 80 K.

Contacts on both YBCO and LSCO samples were prepared in the following way. The contact area was defined using an insulating varnish (GE 7031) (Ref. 10) and was of the order of 0.5 mm×0.5 mm. This was followed by the evaporation of normal-metal layer(s). For samples L1 and Y1–Y4, an aluminum layer of a thickness of 1000 Å was used. For samples Y5, Y6, and Y7, the Al thicknesses were 30, 70, and 100 Å, respectively, followed by the evaporation of 1000 Å of Au. For sample Y8 we evaporated 300 Å Ag followed by 1000 Å Pb on top. The contact on sample L1 was made on the (110) oriented face of the LSCO crystal.

This method of contact preparation usually results in a tunneling junction (samples Y1–Y8) due to oxidation of the first tens of angstroms of the normal-metal layer (see Racah[11]). However, in the LSCO contact (sample L1) a pinhole in the insulating layer was created by voltage breakdown resulting in a small metallic (transparent) contact between the LSCO and the normal metal—this process was suggested and used by Yanson.[12] $I(V)$ characteristics were measured digitally using a current source, and were differentiated using a computer program. Each measurement is comprised of two successive cycles to check the absence of heating-hysteresis effects.

III. RESULTS AND DISCUSSION

YBCO films

A plot of the conductance, representative of group I (sample Y2), is shown in the inset of Fig. 3 at different temperatures. A gaplike feature is seen at about 18 mV, and a ZBCP. Qualitatively, the conductance in all our YBCO samples is characteristic of a contact to a *d*-wave superconductor, with a significant interface barrier, showing a ZBCP followed by a dip, and a return to the normal-state conductance above the gap. The ZBCP is presumably due to surface roughness,[13] associated with the presence of *a*-axis grains and/or holes. At higher temperatures, the gaplike features and the ZBCP are weakened. The ZBCP disappears at a temperature lower than the bulk T_c.

As a test, we used a Pb counter electrode in sample Y8. At 4.2 K, the energy gap of Pb could be seen clearly (not shown). This Pb gap feature disappears as the temperature is

raised above the T_c of Pb, and then the ZBCP appears. This demonstrates that the ZBCP is due to tunneling from a normal metal into the HTS.

In Fig. 3 we present the height of the ZBCP at various temperatures normalized with the height of the ZBCP at 4.2 K, for samples for which the ZBCP disappears around 60 K. We note that the temperature dependence of the ZBCP height is the same for all these YBCO samples, belonging to group I (samples Y1–Y4) and to group II (sample Y5). The ZBCP vanishes well below the films' T_c's (close to 90 K). Following Racah,[11] the smaller T_c of the junction is due to the fact that the Al film is oxidized through the diffusion of oxygen from the HTS film. It is a measure of underdoping of the film near the junction, which is a function of both Al thickness and time elapsed after junction fabrication. Samples Y1–Y4 were measured sooner after fabrication than samples Y5–Y7; therefore, although Samples Y5 and Y1–Y4 have different A1 thickness, they exhibit approximately the same contact T_c.

The conductance versus voltage for samples Y5, Y6, and Y7, prepared and measured simultaneously, is presented in Figs. 4(a), (b), and (c), respectively. In these samples we used Al layers of various thicknesses: 35 Å (Y5), 70 Å (Y6), and 100 Å (Y7). Racah *et al.*[11] have shown that a thin layer (few nm) of Al deposited on top of the YBCO film is oxidized due to oxygen coming from the YBCO film. By increasing the thickness of the thin Al layer we expect two effects: first, a reduction of the barrier transparency, and second, a reduction of the local oxygen doping in the vicinity of the junction.

The conspicuous manifestation of the first effect is the increase of junction resistance with the increasing Al thickness; the junction's resistances at 20 mV and 4.2 K are 0.15, 0.3, and 6 Ω for Samples Y5, Y6, and Y7, respectively. Another observation is the rising linear background which is absent in sample Y5 and which increases with barrier thickening. We relate this background to tunneling into the *c* direction.[14] In the case of a thin Al layer the barrier is almost transparent and the electrons tunnel with a wide momentum cone, and hence the *c*-axis inelastic tunneling effects are not significant. As the barrier becomes thicker the momentum cone around the *c* direction becomes narrower, and hence the *c*-axis inelastic tunneling effects become more important, giving rise to an increasing linear background.[15]

In Fig. 5 one can observe the result of the second effect, the reduction of the local oxygen doping in the vicinity of the junction. Here we plot the ZBCP at different temperatures normalized with the ZBCP at 4.2 K for different Al thicknesses. The temperature above which we could not detect any ZBCP decreased with increasing Al thickness, as expected.[11]

A correlation between surface morphology, as seen from the SEM pictures, and the conductance characteristics is found. When a significant number of *a*-axis grains are present [Fig. 2(a)] the gaplike features at about 18 mV are clearly visible (inset Fig. 3), while in the case of samples Y5–Y7 [Fig. 2(b)] they can hardly be seen [Figs. 4(a)–4(c)]. In Fig. 6 the data of sample Y5 ($T_c \approx 60$ K) are fitted to a $d_{x^2-y^2}$ gap, with the following parameters, using the notation of Kashiwaya *et al.*[3]: $Z=2$, $\Delta=17$ meV, $\alpha=19°$. Here Z is a barrier parameter for a delta function barrier of height H and a Fermi velocity v_f, $Z=(H/hv_f)$, Δ is the amplitude of the *d*-wave gap, and α is the angle between the plane of the interface and the [100] axis. We have also assumed a second conductance channel of 4.5 S corresponding to the dominant *c*-axis tunneling channel.

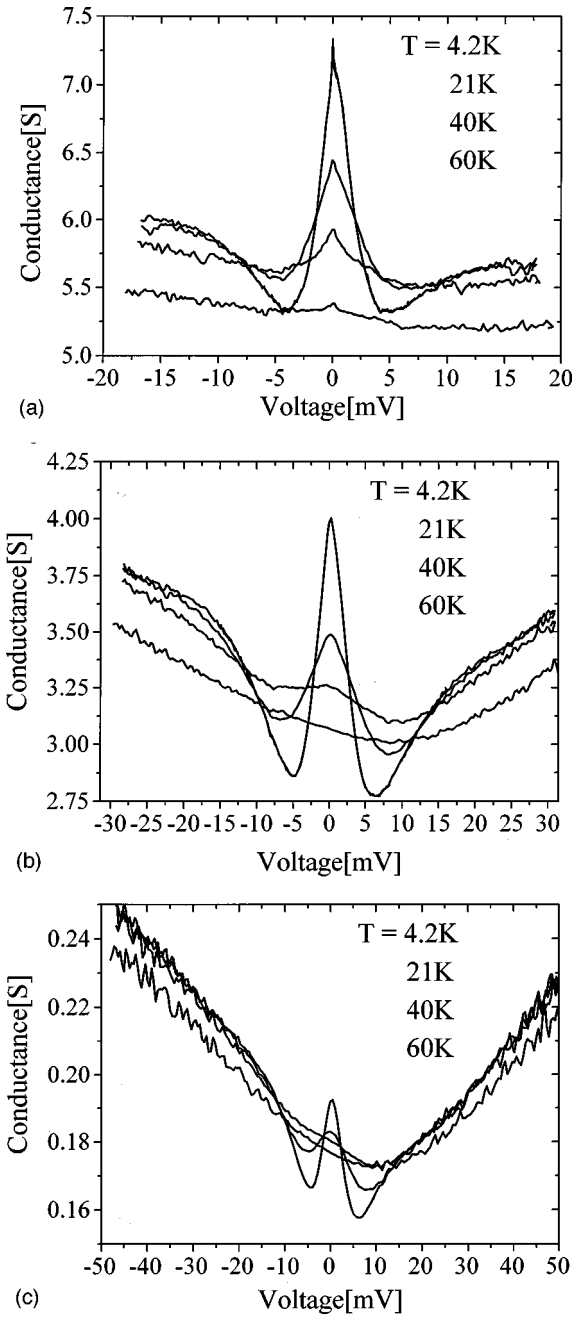

FIG. 4. The conductance versus voltage for different Al thicknesses and at various temperatures. A thicker Al Layer corresponds to a thicker barrier and to a reduced doping in the vicinity of the junction. (a) Sample Y5, 35 Å Al, junction resistance is 0.17 Ω at 20 mV; the ZBCP can be still seen at 60 K and the background is flat. (b) Sample Y6, 70 Å Al, junction resistance is 0.34 Ω at 20 mV; the ZBCP disappears above 40 K. (c) Sample Y7, 100 Å Al, junction resistance is 5 Ω at 20 mV; the ZBCP disappears above 21 K and a rising linear background is seen.

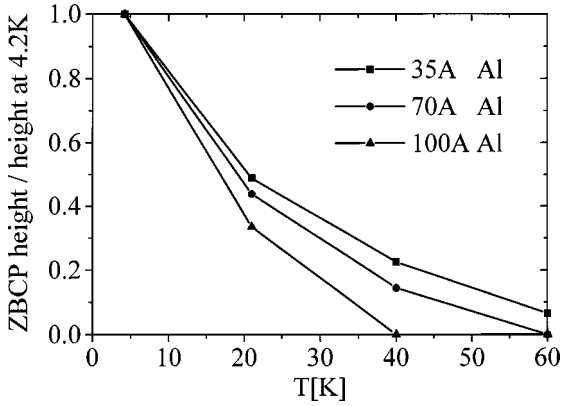

FIG. 5. The ZBCP height at different temperatures normalized with the ZBCP height at 4.2 K for different Al thicknesses. A thicker Al layer corresponds to a reduced doping at the contact; consequently, the ZBCP vanishes more rapidly.

LSCO single crystal

The differential conductance of sample L1 is shown in Fig. 7. It is qualitatively different from that of the YBCO samples: There is no dip in the conductance, but rather a monotonous decrease towards the normal state value. This is characteristic of a contact to a *d*-wave superconductor with a rather transparent barrier. While in the YBCO samples the ZBCP is predominantly due to tunneling into Andreev bound states, here we have direct Andreev reflection characteristics. The temperature dependence of the conductance characteristic is shown in the inset of Fig. 8. The 4.2 K data are indeed well fitted to a $d_{x^2-y^2}$ gap, with the following parameters: $Z=0.75$, $\Delta=5$ meV, $\alpha=\pi/4$ (110) direction (see Fig. 7). It should be noted that contrary to the case of the YBCO sample Y5, no parallel conductance channel had to be assumed to obtain a good fit. The temperature dependence of the ZBCP's height, normalized to its height at 4.2 K, is shown in Fig. 8. The ZBCP height decreases as the temperature is raised, and essentially disappears at about 16 K. Above 16 K, a small remnant peak (not shown) of about 0.5% of the 4.2 K peak, remains approximately constant up to 28 K. It may not be a result of Andreev reflections above

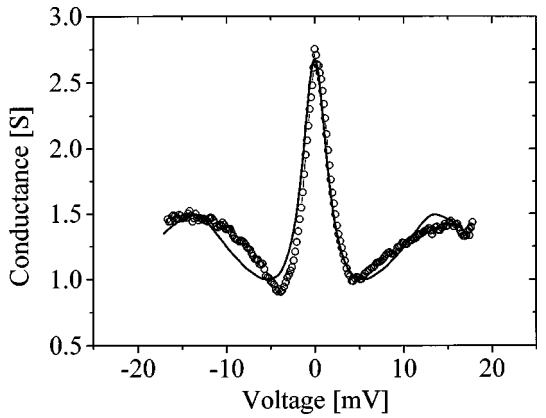

FIG. 6. Measured conductance, sample Y5 (YBCO), at $T=4.2$ K assuming a second conductance channel of 4.5 S corresponding to the dominant *c*-axis tunneling (circles). Theoretical fit to $d_{x^2-y^2}$ gap symmetry: $Z=2$, $\Delta=18$ meV, $\alpha=19°$ (using the notation of Ref. 3) at $T=4.2$ K (solid line).

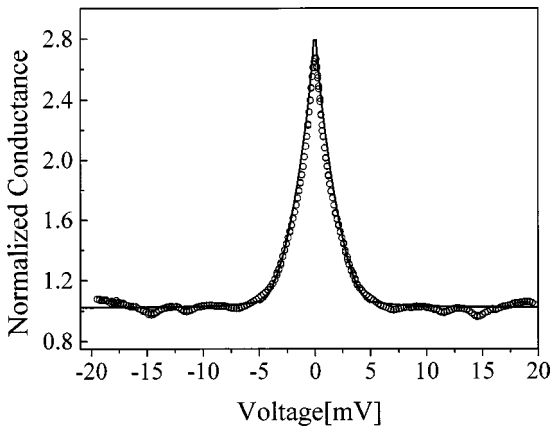

FIG. 7. Measured conductance, sample L1 (LSCO), at $T=4.2$ K normalized with the conductance at 20 mV, 0.023 S (circles). Theoretical fit to $d_{x^2-y^2}$ gap symmetry: $Z=0.75$, $\Delta=5$ meV, $\alpha=\pi/4$ (110) direction (using the notation of Ref. 3) at $T=0$ (solid line).

T_c, but rather a critical current effect. (The bulk T_c of the LSCO crystal is 31 K.) We note that the gap values obtained for the YBCO and LSCO samples roughly fit the respective T_c values.

IV. CONCLUSIONS

A feature common to all our samples is that there are no signs of Andreev reflection above a certain temperature T_c^*, which is always lower than that of the bulk T_c. This holds true for direct Andreev reflections (sample L1) as well as for Andreev bound states (samples Y1–Y8). We have argued that T_c^* is the actual critical temperature of the junction, depressed from its bulk value due to diffusion of oxygen from the HTSC to the metal in contact,[11] as already mentioned. In most of our YBCO samples, the ZBCP disappears at a temperature close to 60 K; this is reasonable, taking into account the plateau in the relation between the YBCO T_c and the doping.[16]

In both YBCO and LSCO samples, the height of the ZBCP saturates at low temperatures. At intermediate temperatures $0.25<T/T_c<0.5$ it can be fitted to a $1/T$ dependence.[17,18] At higher temperatures, the decrease of the

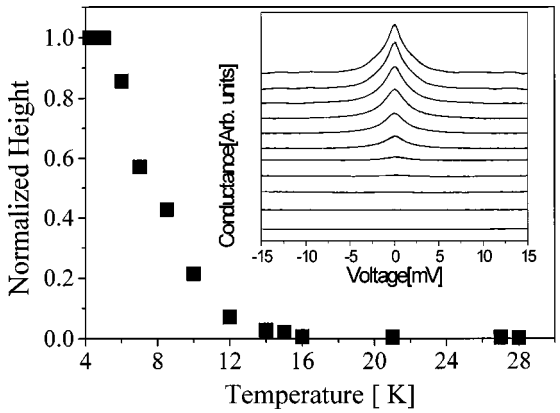

FIG. 8. Height of the ZBCP at various temperatures normalized with the height of the ZBCP at 4.2 K for sample L1. (LSCO) Inset: Conductance for sample L1 at $T=4.2$, 5, 6, 7, 8.5, 10, 12, 14, 15, 27, and 28 K. The graphs were shifted for clarity.

ZBCP height is faster than $1/T$, presumably because of the decrease of the gap value.

When comparing our results to those of Renner *et al.*,[4] we note that in their case the gaplike features persist above T_c. Deutscher[19] has recently shown that Andreev reflection and tunneling measurements correspond to different energy scales; the Andreev scale measured at low temperature following the doping dependence of T_c. This is consistent with the observation reported here, that the Andreev features disappear at the T_c of the junction. We also note that the Andreev gap values obtained from the fits performed on the YBCO (Y5) and LSCO (L1) junctions, scale with the respective junctions T_c.

Choi *et al.*[8] have predicted that, if preformed pairs exist above T_c they should manifest themselves in direct Andreev reflections or Andreev bound states, depending on the transparency of the interface. If this prediction is correct, we should conclude that there are no such pairs above T_c.

ACKNOWLEDGMENTS

We acknowledge useful conversations with Ralph Krupke. This work was supported in part by the Heinrich Hertz–Minerva Center for High Temperature Superconductivity, by a grant from DARPA and ONR, and by the Oren Family Chair of Experimental Solid State Physics.

[1] A. F. Andreev, Zh. Eksp. Eksp. Teor. Fiz. **46**, 1823 (1964) [Sov. Phys. JETP **19**, 1128 (1964)].
[2] G. E. Blonder, M. Tinkham, and T. M. Klapwijk, Phys. Rev. B **25**, 4515 (1982).
[3] S. Kashiwaya, Y. Tanaka, M. Koyanagi, H. Takashima, and K. Kajimura, Phys. Rev. B **51**, 1350 (1995).
[4] C. Renner, B. Revaz, J. Y. Genoud, K. Kadowaki, and Ø. Fischer, Phys. Rev. Lett. **80**, 149 (1998).
[5] I. Chang, J. Friedel, and M. Kohmoto, cond-mat/9908214 (unpublished).
[6] Q. Chen *et al.*, Phys. Rev. Lett. **81**, 4708 (1998).
[7] V. J. Emery and S. A. Kivelson, Phys. Rev. Lett. **74**, 3253 (1995).
[8] H. Choi, Y. Bang, and D. K. Campbell, cond-mat/9902125 (unpublished).
[9] R. Krupke, Z. Barkay, and G. Deutscher, Physica C **315**, 99 (1999).
[10] B. L. Blackford and R. H. March, Phys. Rev. **186**, 397 (1969).
[11] D. Racah and G. Deutscher, Physica C **263**, 218 (1996).
[12] I. K. Yanson, Zh. Eksp. Teor. Fiz. **66**, 1030 (1974) [Sov. Phys. JETP **39**, 506 (1974)].
[13] Y. Tanuma, Y. Tanaka, M. Yamashiro, and S. Kashiwaya, Phys. Rev. B **57**, 7997 (1998).
[14] Y. Dagan *et al.* (unpublished).
[15] P. B. Littlewood and C. M. Varma, Phys. Rev. B **45**, 12 636 (1992).
[16] R. J. Cava, B. Batlogg, C. H. Chen, E. A. Reitman, S. M. Zahurak, and D. Werder, Phys. Rev. B **36**, 5719 (1987).
[17] L. Alff, A. Beck, R. Gross, A. Marx, S. Kleefisch, T. H. Bauch, H. Sato, M. Naito, and G. Koren, Phys. Rev. B **58**, 11 197 (1998).
[18] Yu. S. Barash, A. Svidizinsky, and H. Burkhardt, Phys. Rev. B **55**, 15 282 (1997).
[19] G. Deutscher, Nature (London) **397**, 410 (1999).